Thermoelectric properties and thermopower enhancement of Al-doped ZnO with nanosized pore structure

Ohtaki, Michitaka
Department of Molecular and Material Sciences, Interdisciplinary Graduate School of Engineering Sciences, Kyushu University

Araki, Kazuhiko
Department of Molecular and Material Sciences, Interdisciplinary Graduate School of Engineering Sciences, Kyushu University

出版情報：Journal of the Ceramic Society of Japan. 119 (1395), pp.813-816, 2011-11. 日本セラミックス協会
バージョン：

Journal of the Ceramic Society of Japan 119 [11] 813-816 2011 Paper

Thermoelectric properties and thermopower enhancement of Al-doped ZnO with nanosized pore structure

Michitaka OHTAKI† and Kazuhiko ARAKI

Department of Molecular and Material Sciences, Interdisciplinary Graduate School of Engineering Sciences, Kyushu University, 6–1 Kasugakouen, Kasuga, Fukuoka 816–8580

Thermoelectric properties of Al-doped ZnO ($Zn_{0.98}Al_{0.02}O$) with nanosized pore (nanovoid) structure were investigated. Nanovoids were formed by using monodisperse polymethylmethacrylate (PMMA) particles of 150, 425, and 1800 nm in average diameter as a void forming agent (VFA). Whereas the thermal conductivity of the samples sintered with the 150 nm PMMA particles of 5–10 wt % was efficiently suppressed, the magnitude of the suppression was almost the same as that of the electrical conductivity, revealing that the selective phonon scattering was failed in these samples. However, being helped by the contribution from an enhancement in the Seebeck coefficient, the samples sintered with 5–10 wt % of 150 nm VFA successfully attained the *ZT* values of 0.55–0.57 at 1000°C. Furthermore, the reduction of the thermal conductivity with increasing porosity was much steeper than ordinary porous materials, suggesting significantly stronger phonon scattering by the nanosized pore structure.

Key-words : Thermoelectric material, ZnO, Microstructure, Phonon scattering, Thermal conductivity

[Received July 20, 2011; Accepted August 1, 2011]

1. Introduction

Thermoelectric power generation is expected as a waste heat recovery technology for higher energy efficiency, by which thermal energy is directly converted into electrical energy.[1] Thermoelectric materials having been used in practical are all non-oxides, and much attention is currently being paid to oxide thermoelectric materials from the viewpoint of chemical stability, thermal resistance, environmental safety, and uncostly manufacturing processes.[2),3)]

The thermoelectric performance of materials are evaluated by the figure-of-merit defined as $Z = \sigma S^2/\kappa$, where σ is the electrical conductivity, S is the Seebeck coefficient, and κ is the thermal conductivity. ZnO-based oxide thermoelectric material shows a high electrical performance (power factor, the numerator of Z) sufficiently competitive to conventional materials such as PbTe. However, the overall performance of the oxide has been only about 30 percent ($ZT = 0.3$) of the practical requirement, because the thermal conductivity (the denominator of Z) of the oxide is significantly high.[4)–8)] We are aiming to decrease solely the thermal conductivity without degrading the electrical performance by forming the closed pores of the order of 100 nm (nanovoid) into a dense matrix of $Zn_{0.98}Al_{0.02}O$ (ZnAlO), which composition has been known to show the best thermoelectric performance in the ZnO system.[4),5)] Selective scattering of phonons without affecting electrical transport is an ultimate target in thermoelectric materials research. We have already reported a significant enhancement of the thermoelectric performance of Al-doped ZnO, in which a nanovoid structure has been introduced into a densely sintered ZnAlO matrix by employing combustible nanosized particles as a void forming agent (VFA), resulting in a dimension less figure-of-merit of $ZT = 0.65$ at 1250 K.[9)] However, a decrease in the electrical conductivity (σ) caused by the nanovoid structure was larger than that of the thermal conductivity (κ), resulting in smaller σ/κ ratios; selective enhancement of phonon scattering was unsuccessful, and hence the improved ZT was attributed to an unexpected but considerable increase in the thermopower (S) in the nanovoid samples.

In this paper, we investigate influence of the size and amount of VFA on the thermoelectric properties of the nanovoid ZnO aiming at the selective phonon scattering by the nanovoid structure. We also examine the relation between the porosity and thermal conductivity of the nanovoid samples, in which the relation may differ from those for ordinary porous media.

2. Experimental

2.1 Preparation of samples

Zinc oxide was commercially obtained in reagent grade (>99.9%, Kishida Kagaku). The Al source was γ-Al_2O_3 with low crystallinity, prepared by hydrolyzing Al[*i*-$(C_3H_7)_3$] (>99.9%, Kishida Kagaku) in 2-propanol followed by firing at 500°C in air. Employed as void forming agent (VFA) were monodispersed spherical beads of polymethylmethacrylate (PMMA) with average diameters of 150, 425, and 1800 nm supplied by Soken Chemical & Engineering, Co., Ltd.

The powders of ZnO and γ-Al_2O_3 were weighed at an atomic ratio of Zn:Al = 98:2, and mixed in an conventional polyethylene-lined ball mill for 24 h. The resulting powder was then mixed with 3–10 wt % of VFA with a Fritsch P-6 planetary-type ball mill for 1 min × 3 times, using ϕ 2 mm zirconia beads and water as mixing media. The dried mixture after separation of the zirconia beads was uniaxially pressed into a pellet, then cold isostatic pressed at 110 MPa, and sintered at 1400°C for 5 h in N_2. Al-doped ZnO as the matrix of the samples, $Zn_{0.98}Al_{0.02}O$, is denoted as ZnAlO in this paper.

2.2 Measurement of thermoelectric properties

Measurements of the electrical conductivity, σ, and the Seebeck coefficient, S, were carried out simultaneously from room temperature to 1000°C in air with an Ozawa Science RZ2001i. The σ values were measured by the dc four-probe

† Corresponding author: M. Ohtaki; E-mail: ohtaki@mm.kyushu-u.ac.jp

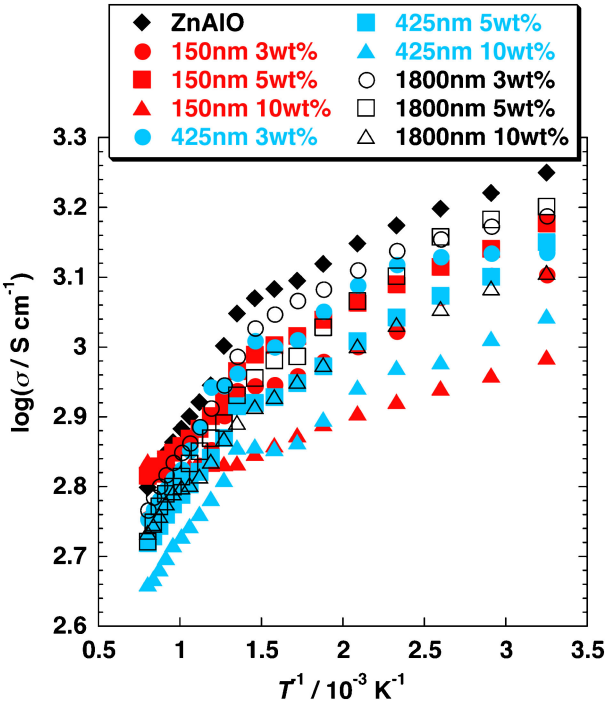

Fig. 1. (Color online) The temperature dependence of the electrical conductivity, σ, of the samples sintered with 0–10 wt% of 150, 425, 1800 nm VFA.

technique. The S values were obtained from the least-squares regressions of the thermoelectromotive force as a function of the temperature difference of <5 K applied at each measurement temperature. The thermal conductivity, κ, was determined from the thermal diffusivity, α, and the specific heat capacity, C_p, measured by the laser flash technique on a Kyoto Electronics LFA-502 as $\kappa = \alpha C_p \rho$, where ρ is the density. The SEM observations of the powder compacts and the cross sections of the sintered samples were carried out on a JEOL JSM-6340F field-emission scanning electron microscope. The density of the samples was measured by the Archimedes' method yielding the apparent density, in which only the closed pores are subject to the measurement.

3. Results and discussion

In order to investigate the influence of the size and amount of VFA on the transport properties of Al-doped ZnO, we have employed VFAs with a variety of size and amount. Since planetary ball mills can apply large pulverizing energy to samples, we limited the mixing time as short as 1 min × 3 times at 600 rpm in order to prevent the defect formation in ZnO, attaining both high σ values and a high dispersion state of VFA.

The temperature dependence of the electrical conductivity, σ, of ZnAlO sintered with the 150, 425, 1800 nm VFA is shown in **Fig. 1**. As expected, the σ values decreased in accordance with the increased size and amount of VFAs. However, the absolute values of S shown in **Fig. 2** significantly increased with decreasing average diameter of VFAs from 1800 nm down to 150 nm.

The temperature dependence of the thermal conductivity, κ, of neat ZnAlO and samples sintered with 150, 425, 1800 nm VFA is shown in **Fig. 3**. The κ values of the samples decreased with increasing size and amount of VFAs, being consistent with a larger porosity expected for these samples. We have hence further examined the decrease in κ in terms of the porosity.

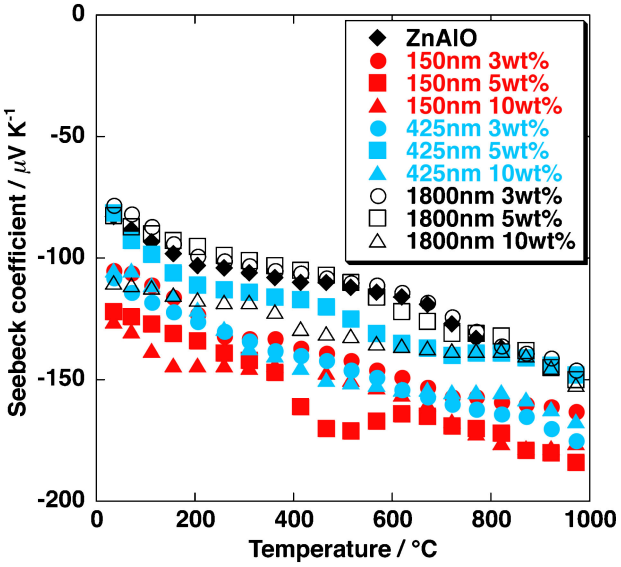

Fig. 2. (Color online) The temperature dependence of the Seebeck coefficient, S, of the samples sintered with 0–10 wt% of 150, 425, 1800 nm VFA.

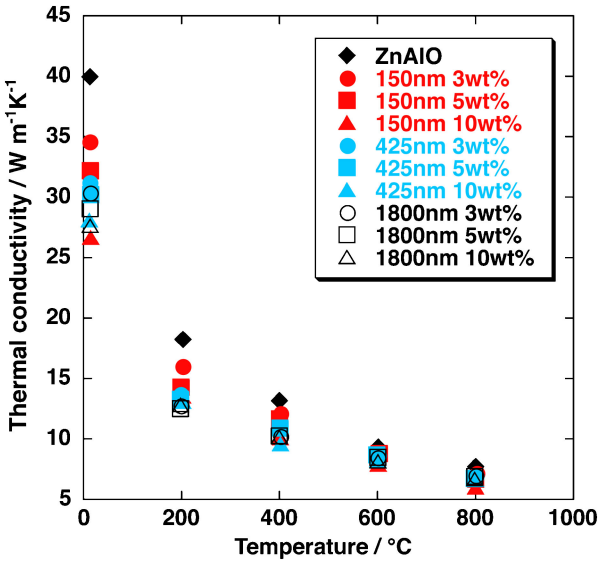

Fig. 3. (Color online) The temperature dependence of the thermal conductivity, κ, of the samples sintered with 0–10 wt% of 150, 425, 1800 nm VFA.

The thermal conductivity of porous materials has extensively been studied on practical heat insulators such as refractory bricks, foam glasses and fibers.[10)–15)] Porous materials are generally divided into two groups: foam-like structures in which voids or pores are dispersed in a solid, and granular or fiber-like structures in which granules or fibers are separated by recesses or layers of air between them. The macroscopic flow of the fluid phase (usually air) can be neglected in the former case except convection flows in large pores, whereas the structures may vastly vary and the fluid phase can flow through the materials in the latter case. Although the radiative thermal conduction across the pores should also be considered at high temperature, this effect becomes significant only for the pores larger than 1 mm at temperatures higher than 700 K for Al_2O_3 with the porosity of 0.5.[16)] With respect to the extremely small pore size and low porosity in this study, influences of the radiative conduction and

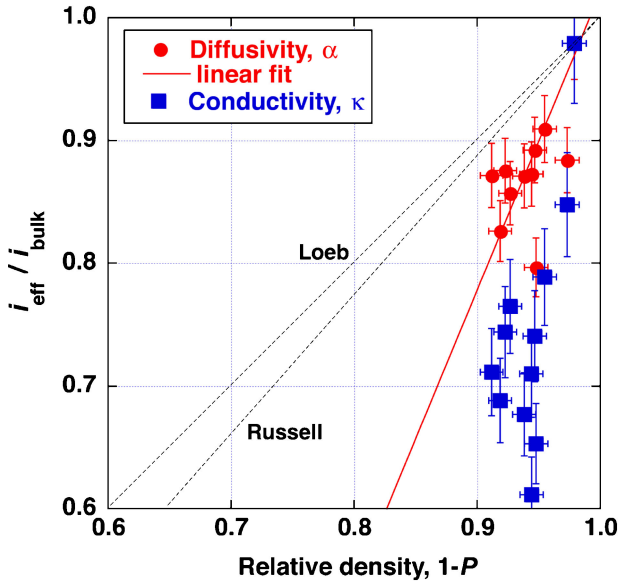

Fig. 4. (Color online) The thermal diffusivity, α, and thermal conductivity, κ, measured at room temperature as a function of the relative density of Al-doped ZnO prepared with various size and amount of VFAs. The dashed lines represent the conventional κ-porosity relations. The error bars are based on the experimental errors of density and thermal diffusivity measurements.

convection flows in the pores can be neglected. For such a simplified model, Russell[12] calculated the thermal conductivity of composites or porous materials (κ_c) with cubic pores (with κ_a) of a total volume of V_a embedded in a solid matrix (with κ_s) with a volume of V_s as

$$\kappa_c = \kappa_s \frac{P^{2/3} + \frac{\kappa_s}{\kappa_a}(1 - P^{2/3})}{P^{2/3} - P + \frac{\kappa_s}{\kappa_a}(1 - P^{2/3} + P)} \quad (1)$$

where the porosity, P, is a volume fraction of pores or voids, defined as $P = V_a/(V_a + V_s)$. It should be noted that for granular or fibrous structures ($\kappa_s < \kappa_a$), the κ_c values are given by the same type of equation, Eq. (1) being modified by replacing P by $(1 - P)$ and interchanging κ_s and κ_a.

For the foam-like structures consisting of hollow cells with solid walls ($\kappa_s \gg \kappa_a$), the κ_c values calculated by Eq. (1) decreases virtually in proportion to the relative density, $1 - P$, as seen in the literature.[12] However, as shown in **Fig. 4**, conventional κ-porosity relations, i.e. by Russell[12] or Loeb,[13] are revealed to no longer hold for nanovoid structure in the present study. Even the nanovoid Al-doped ZnO showed almost linear decreases in α and κ with increasing porosity, the slopes against the relative density were remarkably much steeper than the conventional predictions. These results suggest that the nanovoid structure in this study is capable of scattering phonons much more strongly compared to conventional porous structures at the same porosity. Consequently, as shown in **Fig. 5**, $ZT = 0.55$–0.57 at 1000°C was obtained for the samples prepared with 5–10 wt% of 150 nm VFA.

Finally, **Fig. 6** depicts the relative increase/decrease in $|S|$, σ, and κ for the sample sintered with 5 wt% of 150 nm VFA, normalized by those of the dense mother phase ZnAlO. Since the decrease in σ was in the same magnitude as that in κ, selective phonon scattering[17),18)] was revealed to fail at the present moment. However, the Seebeck coefficient increased significantly over the

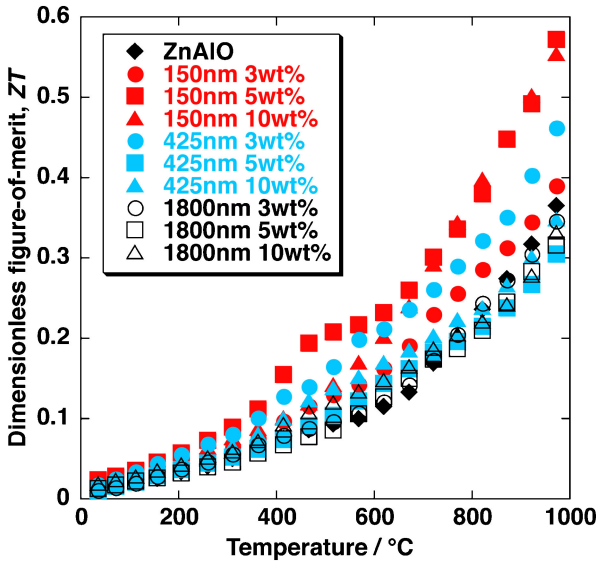

Fig. 5. (Color online) The temperature dependence of the dimensionless-figure-of-merit, ZT, of the samples sintered with 0–10 wt% of 150, 425, 1800 nm VFA.

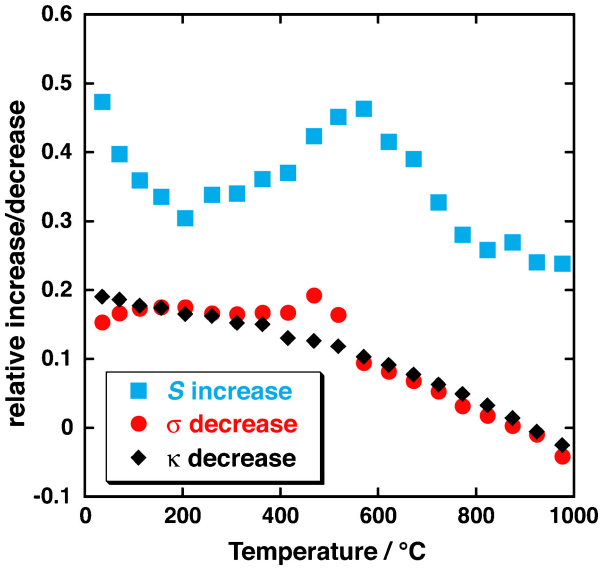

Fig. 6. (Color online) The relative increase/decrease of S, σ, and κ for the sample sintered with 5 wt% of 150 nm VFA normalized by those of the mother phase ZnAlO. Note that the relative values of the increase in $|S|$ and the decreases in σ and κ are plotted in the positive direction.

whole temperature range by introducing the nanosized pores, resulting in a marked improvement in the dimensionless figure-of-merit. Unfortunately, the nature of the enhancement in S is still an open question, while energy filtering of low-energy carriers due to low-energy defects associated with the nanovoids is implied.

In order to elucidate the mechanism of the present enhancement in the thermoelectric performance of the nanovoid oxides, further investigation particularly on shape, size distribution, and surface/boundary structures of the nanovoids is absolutely necessary.

4. Conclusions

Nanosized pore (nanovoid) structure was confirmed to be effective for improving the thermoelectric performance of bulk Al-doped ZnO, attaining $ZT = 0.57$. Although the nanovoid

structure in this study appears to be still far from optimal, highly dispersed nanosized closed pores (nanoviods) were confirmed to be effective for improving the thermoelectric performance of bulk Al-doped ZnO, attaining $ZT = 0.55$–0.57 as the largest values so far reported for bulk Al-doped ZnO.

The κ reduction of the nanovoid samples was revealed to be much more intense compared to ordinary porous materials, suggesting an unconventional phonon scattering mechanism. Although the nanostructure in this study appears to be still far from optimal, an importance of shape, size distribution, and surface/boundary structure is suggested to be strongly important for phonon scattering by the nanovoid structure.

References

1) "CRC Handbook of Thermoelectrics", Ed. by M. D. Rowe, CRC Press, Inc., Boca Raton, USA (1995) ISBN 0-8493-0146-7.
2) "Oxide Thermoelectrics", Ed. by K. Koumoto, I. Terasaki and N. Murayama, Research Signpost, Trivandrum, India (2002) ISBN 81-7736-100-7.
3) M. Ohtaki, *J. Ceram. Soc. Japan*, **119**(11), in press (2011).
4) M. Ohtaki, T. Tsubota, K. Eguchi and H. Arai, *J. Appl. Phys.*, **79**, 1816–1818 (1996).
5) T. Tsubota, M. Ohtaki, K. Eguchi and H. Arai, *J. Mater. Chem.*, **7**, 85–90 (1997).
6) T. Tsubota, M. Ohtaki, K. Eguchi and H. Arai, Proc. 16th Int. Conf. Thermoelectrics, IEEE, Piscataway (1997) p. 240–243.
7) T. Tsubota, M. Ohtaki, K. Eguchi and H. Arai, *J. Mater. Chem.*, **8**, 409–412 (1998).
8) M. Ohtaki, T. Tsubota and K. Eguchi, Proc. 17th Int. Conf. Thermoelectrics, IEEE, Piscataway (1998) p. 610–613.
9) M. Ohtaki and R. Hayashi, Proc. 25th Int. Conf. Thermoelectrics, IEEE, Piscataway (2006) p. 276–279.
10) A. Eucken, *VDI-Forschungsh.*, **B3**, No. 353, 1–16 (1932).
11) J. Francl and W. D. Kingery, *J. Am. Ceram. Soc.*, **37**, 99–107 (1954).
12) H. W. Russell, *J. Am. Ceram. Soc.*, **18**, 1–5 (1935).
13) A. L. Loeb, *J. Am. Ceram. Soc.*, **37**, 96–99 (1954).
14) T. Kunii, *Chem. Eng.*, **25**, 891–898 (1961) [in Japanese].
15) T. Saegusa, K. Kamata et al., *Chem. Eng.*, **37**, 811–814 (1973) [in Japanese].
16) T. Kunii, "Thermal Unit Operations", Maruzen, Tokyo (1976) p. 126 [in Japanese].
17) C. B. Vining, *J. Appl. Phys.*, **69**, 331–341 (1991).
18) G. A. Slack and M. A. Hussain, *J. Appl. Phys.*, **70**, 2694–2718 (1991).